

Expanding the Reach of Heavy Neutrino Searches at the LHC

Andrés Flórez², Kaiwen Gui¹, Alfredo Gurrola¹, Carlos Patiño², and Diego Restrepo³

¹ Department of Physics and Astronomy, Vanderbilt University, Nashville, TN, 37235, USA

² Physics Department, Universidad de los Andes, Bogotá, Colombia

³ Department of Physics, Universidad de Antioquia, Medellín, Colombia

(Dated: November 27, 2024)

The observation of neutrino oscillations establishes that neutrinos (ν_ℓ) have non-zero mass and provides one of the more compelling arguments for physics beyond the standard model (SM) of particle physics. We present a feasibility study to search for hypothetical Majorana neutrinos (N_ℓ) with TeV scale masses, predicted by extensions of the SM to explain the small but non-zero ν_ℓ mass, using vector boson fusion (VBF) processes at the 13 TeV LHC. In the context of the minimal Type-I seesaw mechanism (mTISM), the VBF ℓN_ℓ production cross-section surpasses that of the Drell-Yan process at approximately $m_{N_\ell} = 1.4$ TeV. We consider μN_μ and τN_τ production through VBF processes (e.g. $qq' \rightarrow \tau N_\tau qq'$), with subsequent N_μ and N_τ decays to μjj and τjj , as benchmark cases to show the effectiveness of the VBF topology for N_ℓ searches at the 13 TeV LHC. The requirement of a dilepton pair combined with four jets, two of which are identified as VBF jets with large separation in pseudorapidity and a TeV scale dijet mass, is effective at reducing the SM background. This criteria may provide expected exclusion bounds, at 95% confidence level, of $m_{N_\ell} < 1.7$ (2.4) TeV, assuming 100 (1000) fb^{-1} of 13 TeV data from the LHC and mixing $|V_{\ell N_\ell}|^2 = 1$. The use of the VBF topology to search for m_{N_ℓ} increases the discovery reach at the LHC, with expected significances greater than 5σ (3σ) for N_ℓ masses up to 1.7 (2.05) TeV using 1000 fb^{-1} of 13 TeV data from the LHC.

I. INTRODUCTION

The discovery of a Higgs boson [1, 2] at the Large Hadron Collider (LHC) has addressed the last missing piece of the standard model (SM) of particle physics. However, the SM remains an incomplete theory. One of the open questions it fails to address is the non-zero mass of the three generations of neutrinos, which is implied by the observation of neutrino oscillations [3–5]. It has been suggested that because neutrinos can be their own anti-particles (Majorana fermions), the non-zero mass of light neutrinos ν_ℓ could be generated by a see-saw mechanism [6–8], which would imply the existence of yet unobserved heavier Majorana neutrino states with TeV scale masses. For example, in the left-right symmetric model (LRSM), originally introduced to explain the non-conservation of parity in weak interactions within the SM, the introduction of a $\text{SU}(2)_R$ group, the right-handed analogue of the SM $\text{SU}(2)_L$ group, produces three heavy right-handed neutrino states N_ℓ ($\ell = e, \mu, \tau$) and three gauge bosons, $V_R = \{W_R^\pm, Z'\}$.

The CMS [9] and ATLAS [10] experiments at the CERN LHC have a strong physics program to search for heavy right-handed neutrinos. One often used benchmark model in those searches is the LRSM. Within this context, the CMS and ATLAS searches assume that N_ℓ is lighter than V_R : $m_{N_\ell} < m_{W_R^\pm}$ and $m_{N_\ell} < 0.5m_{Z'}$. Under this assumption, the dominant N_ℓ production mechanism at the LHC is via resonant W_R^\pm or Z' production from Drell-Yan (DY) processes of order α_{EW}^2 : $qq' \rightarrow W_R^\pm \rightarrow \ell N_\ell$ or $q\bar{q} \rightarrow Z' \rightarrow N_\ell N_\ell$. The strategy pursued in those analyses is to exploit the high mass scale of V_R and target the N_ℓ decay to a lepton and two jets (through a virtual W_R), $N_\ell \rightarrow \ell W_R^* \rightarrow \ell jj$, by selecting

events containing two high- p_T leptons (opposite-sign or like-sign charge) and two jets that are central in the detector (i.e. pseudorapidity range $|\eta| < 3.0$). Therefore, dilepton triggers can be used to select signal events with high efficiency. Furthermore, because DY-like production of resonant W_R^\pm or Z' is dominant if $m_{N_\ell} < m_{W_R^\pm}$ or $m_{N_\ell} < 0.5m_{Z'}$, the invariant mass distribution of the system consisting of two high- p_T leptons and jets, $m_{\ell\ell\Sigma j}$, produces a "bump" in signal events, at $m_{\ell\ell\Sigma j} \approx m_{V_R}$, which can be utilised to discriminate against the smooth and steeply falling SM background distribution. Results of those searches in proton-proton collisions at $\sqrt{s} = 7, 8$, and 13 TeV exclude N_ℓ masses below 1.5 (0.8 TeV) [11–13], assuming m_{N_ℓ} is 0.5 (0.4) times the mass of the W_R (Z') boson. However, the sensitivity to N_ℓ is dependent on the mass of the W_R^\pm or Z' bosons. For example, no bounds on m_{N_ℓ} exist for $m_{W_R^\pm} (m_{Z'}) \sim m_{N_\ell}$ ($2m_{N_\ell}$). Additionally, if the W_R^\pm and Z' bosons are too heavy to provide large enough cross-section, regardless of m_{N_ℓ} , another technique must be devised to probe N_ℓ . For this reason, the CMS and ATLAS experiments also perform more general and less model-dependent searches by considering the simplest extension to the SM which can explain the small but non-zero mass of ν_ℓ , the so-called minimal Type-I seesaw mechanism (mTISM). In this model, the only additional degrees of freedom beyond the SM are the heavy Majorana neutrinos. Therefore, the N_ℓ is produced through an off-mass-shell W boson, $qq' \rightarrow W^* \rightarrow \ell N_\ell$. Although the ℓjj final state particles are similar to the case of the LRSM, the kinematics are different. In the mTISM final state, because the first lepton is produced by an off-mass-shell W boson, $p_T(\ell)$ is significantly smaller on average than in the LRSM final state. Also, because the jets are produced by an on-

mass-shell W boson ($N_\ell \rightarrow \ell W \rightarrow \ell jj$), the dijet mass is consistent with m_W . Results of the mTISM searches depend on the mixing between N_ℓ and ν_ℓ , $|V_{\ell N_\ell}|^2$, and exclude $m_{N_\ell} < 500$ (200) GeV for $|V_{\ell N_\ell}|^2 = 1$ (10^{-2}).

The focus of this paper is to explore production of N_ℓ via vector boson fusion (VBF) processes and the effectiveness of the VBF topology for N_ℓ searches at the 13 TeV LHC. A search for N_ℓ using the VBF topology has not been performed before at a collider, but may present an important avenue for discovery. The VBF topology is characterized by two high p_T forward jets (j_f), with large pseudorapidity gap, located in opposite hemispheres of the detector, and TeV scale dijet invariant masses. The tagging of events produced through VBF processes has been proposed by some of the present authors as an effective experimental tool for dark matter (DM) and electroweak supersymmetry (SUSY) searches at the LHC [14–18], as well as searches for a TeV scale neutral gauge boson Z' [19]. A comparison with current results from CMS and ATLAS is performed in the most model-independent setting by using the mTISM model as the benchmark scenario. To highlight the usefulness of the VBF topology in N_ℓ searches with large QCD backgrounds as well as those with cleaner signatures, we consider $\mu N_\ell jjjj$ and $\tau N_\ell jjjj$ production through VBF processes with subsequent N_ℓ and N_τ decays to μjj and τjj , respectively. In the VBF N_τ study, we focus on the final state where both τ leptons decay to hadrons (τ_h) since it provides the largest branching fraction (42%) compared to final states with semi-leptonic decays of τ leptons. Therefore, the final states considered in this paper are $\mu jjjjjj$ and $\tau_h \tau_h jjjjjj$, where j refers to a jet not tagged as a VBF jet. Figure 1 shows an example Feynman diagram for the production mechanism of N_τ , in particular $W\gamma$ fusion in t-channel diagrams containing an off-mass shell W boson. The N_τ subsequently decays to a τ lepton and two jets.

II. SAMPLES AND SIMULATION

The SM background and N_ℓ signal event samples were generated with MadGraph (v2.2.3) [20]. We considered two sets of signal samples: (i) $pp \rightarrow \mu N_\ell jjjj$, and (ii) $pp \rightarrow \tau N_\tau jjjj$ via pure electroweak VBF processes of order α_{EW}^4 . The N_ℓ masses considered range from 0.5 TeV to 3 TeV in steps of 0.25 TeV. At the MadGraph level, leptons were required to have a $p_T(\ell) > 10$ GeV and $|\eta(\ell)| < 2.5$, while jets were required to have a minimum $p_T > 20$ GeV and $|\eta| < 5.0$. Figure 2 shows a comparison of the $pp \rightarrow \tau N_\tau$ (DY-like) and $pp \rightarrow \tau N_\tau jjjj$ (VBF) production cross-sections as a function of m_{N_τ} . At the 13 TeV LHC, the VBF ℓN_ℓ production cross-section surpasses that of the DY process at approximately $m_{N_\ell} = 1.4$ TeV. We note the $pp \rightarrow \mu N_\ell jjjj$ production cross-section is similar to the $pp \rightarrow \tau N_\tau jjjj$ cross-section shown in Figure 2 as long as the mixing parameters are equal.

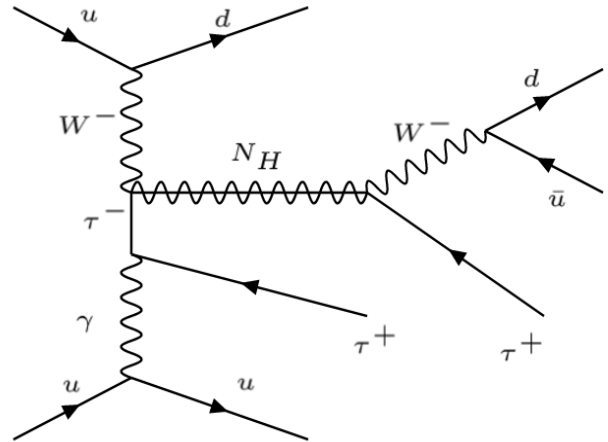


FIG. 1. Feynman diagram depicting pure electroweak production of a N_ℓ particle through VBF.

The dominant sources of background in these studies are the production of top quark pairs with associated jets from initial state radiation (ISR) processes ($t\bar{t}$), $Z/\gamma^* \rightarrow \ell\ell$ with associated jets mostly from ISR (Z +jets), and events with a W boson and ISR jets (W +jets). Samples of events from the production of pairs of vector bosons (VV) were also considered as a potential source of background, but were found to be negligible after the signal selection criteria outlined in subsequent sections. For this reason they are not included in the figures. Background from $t\bar{t}$ events is characterised by two b quark jets from the decays of the top quarks, two real prompt isolated leptons from the decay of a W boson ($t \rightarrow bW \rightarrow b(\ell\nu_\ell)$), and two additional jets from initial state radiation. Although Z +jets events can be produced through VBF processes, the requirement of four jets in the final state suppresses the VBF Z contribution and makes Z production with associated ISR jets the dominant contribution to the Z +jets background. Since the Z/γ^* bosons can subsequently decay to real leptons, the topology of this background includes two real leptons and four additional ISR jets, two of which are in the forward parts of the detector. In the case of W +jets events, which is only relevant for the $\tau_h \tau_h jjjjjj$ final state, a real prompt lepton is obtained from the decay of the W boson and the second τ_h results from the misidentification of a jet as a τ_h .

PYTHIA (v6.416) [21] was used for the hadronization process of the signal and background samples. The Delphes (v3.3.2) [22] framework was used to simulate detector effects using the CMS configuration. The $t\bar{t}$ background sample was generated with up to two associated jets, while the Z +jets and W +jets samples were generated with up to four associated jets, inclusive in α_{EW} and α_{QCD} . The MLM algorithm [23] was used for jet

matching and jet merging, which optimizes two variables (xqcut and qcut) related to the jet definition. The xqcut variable defines the minimal distance between partons at MadGraph level. The qcut variable defines the minimum energy spread for a clustered jet in PYTHIA. In order to determine appropriate xqcut and qcut values, the distribution of the differential jet rate was required to smoothly transition between events with N and $N+1$ jets. The jet matching and merging studies resulted in an optimized xqcut and qcut of 30.

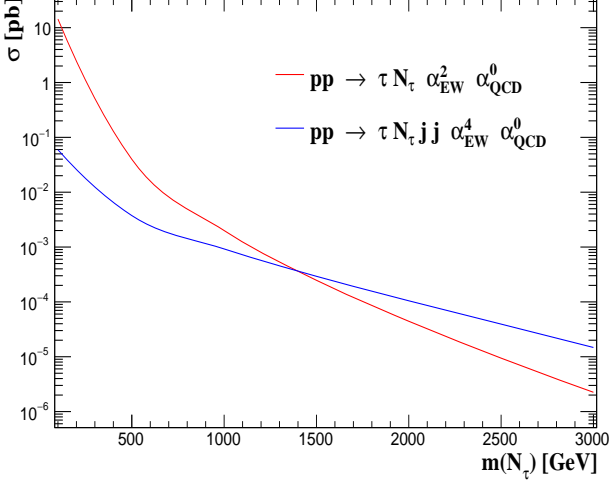


FIG. 2. N_ℓ production cross-section as a function of mass. The VBF N_ℓ production cross-section exceeds the production via the DY process at approximately $m_{N_\ell} = 1.4$ TeV.

III. EVENT SELECTION CRITERIA

The event selection criteria used in these studies are divided in two parts, referred to as central selections and VBF selections. The central selections include requirements on the transverse momentum of the leptons and jets ($p_T(\ell/j) > X$), the geometric acceptance pseudorapidity requirements ($|\eta(\ell/j)| < Y$), the absolute value of the scalar difference in p_T between the two lepton candidates ($\Delta p_T = |p_T^{\ell_1} - p_T^{\ell_2}|$), the product of the electric charges of the two leptons ($Q(\ell_1) \times Q(\ell_2)$), and a veto on the number of jet candidates identified as b-quarks ($N_b = 0$). Since our focus is high-mass N_ℓ , signal events are characterized by one high- p_T lepton ($p_T(\ell) \sim \frac{1}{3}m_{N_\ell}$). Therefore, the highest- p_T lepton in the event is required to have $p_T > 50$ GeV, which helps to drastically reduce events from Z +jets and W +jets processes (e.g. $p_T(\tau_h) \sim m_W/4 = 20$ GeV in W +jets events). The p_T cut on the second lepton is driven by the experimental constraints of the CMS and ATLAS reconstruction algorithms. The sub-leading muon must have $p_T > 10$ GeV, while the sub-leading τ_h must have

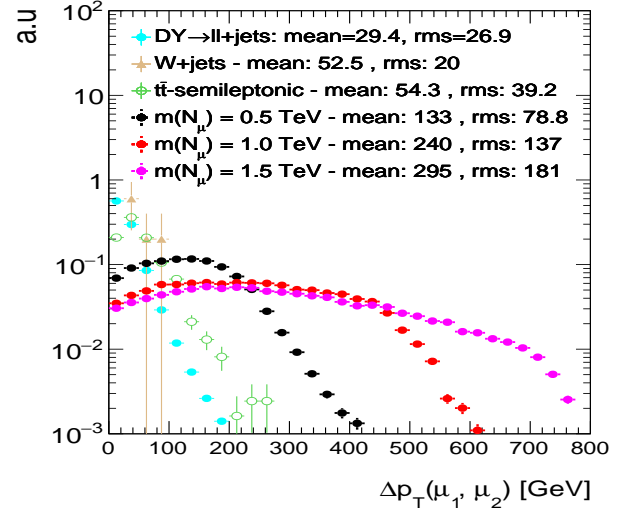


FIG. 3. Δp_T distributions, normalized to unity, for the $\mu\mu jj jj jj$ final state. The distributions are obtained after requiring at least two muons with $p_T > 10$ GeV and $|\eta| < 2.4$.

$p_T > 20$ GeV. Events are required to have at least four jets, two of which are considered central jets. The pseudorapidity is constrained to $|\eta| < 2.4$ (2.1) for muons (τ_h) and $|\eta| < 2.4$ for central jets, which allows these objects to be within the tracker coverage of the detector, thus improving reconstruction efficiency. In background events, the leptons mainly come from decays of W bosons (e.g. $t\bar{t} \rightarrow b\bar{b}WW \rightarrow b\bar{b}\ell\nu_\ell\ell\nu_\ell$) and Z/γ^* bosons ($Z \rightarrow \ell\ell$), and therefore both leptons have a similar p_T on average, i.e. $p_T(\ell_1) \approx p_T(\ell_2)$. On the other hand, because the first lepton in signal events is produced via non-resonant t-channel $W\gamma$ fusion diagrams (making it low- p_T) and the second lepton is produced by the decay of a heavy on-mass shell N_ℓ (making it high- p_T), the p_T values of the two leptons are largely asymmetric. This motivates a requirement on the absolute value of the scalar difference in p_T between the two leptons. Figure 3 shows the $\Delta p_T = |p_T^{\ell_1} - p_T^{\ell_2}|$ distribution for the $\mu\mu jj jj jj$ final state, normalized to unity, for two signal benchmark points and the main backgrounds. A $\Delta p_T = |p_T^{\ell_1} - p_T^{\ell_2}| > 50$ GeV criterion helps to suppress approximately 80% of the SM background, while maintaining about a 90% efficiency for signal events. A same-sign charge requirement between the two leptons, $Q(\ell_1) \times Q(\ell_2) > 0$, reduces the Z +jets background by two orders of magnitude and is over 95% efficient for signal. Finally, requiring events with zero jets tagged as b-quarks suppresses 80% of the $t\bar{t}$ background, while being $\sim 90\%$ efficient for signal events.

The distinctive signature of VBF processes is the presence of two high- p_T jets, with a large pseudorapidity gap ($|\Delta\eta|$), and located in opposite hemispheres of the detector. The invariant mass of the $j fj f$ pair, especially for signal, is expected to be broad and fall at TeV scale val-

TABLE I. Event selection criteria for the $\mu\mu/\tau\tau + jjjj_{ff}$ channels.

Criterion	$\tau_h\tau_h jjjj_{ff}$	$\mu\mu jjjj_{ff}$
Central Selections		
$ \eta(\tau_h/\mu) $	< 2.1	< 2.4
$p_T^{lead}(\tau_h/\mu)$	> 50 GeV	> 50 GeV
$p_T^{slead}(\tau_h/\mu)$	> 20 GeV	> 10 GeV
$N(\tau_h/\mu)$	≥ 2	≥ 2
$\Delta R(\tau_{h1}/\mu_1, \tau_{h2}/\mu_2)$	> 0.3	> 0.3
$ \Delta p_T(\tau_{h1}/\mu_1, \tau_{h2}/\mu_2) $	> 50 GeV	> 50 GeV
$Q(\tau_{h1}/\mu_1) \times Q(\tau_{h2}/\mu_2)$	> 0	> 0
N_{b-jets}	$= 0$	$= 0$
$p_T^{central}(j)$	30 GeV	30 GeV
$ \eta^{central}(j) $	< 2.4	< 2.4
$N_{central}(j)$	$= 2$	$= 2$
$\Delta R(\tau_h/\mu, j)$	> 0.4	> 0.4
VBF Selections		
$p_T^{lead}(j_f)$	30 GeV	30 GeV
$ \eta^{lead}(j_f) $	< 5.0	< 5.0
$p_T^{sub-lead}(j_f)$	30 GeV	30 GeV
$ \eta^{sub-lead}(j_f) $	< 5.0	< 5.0
$\Delta R(\tau_h/\mu, j_f)$	> 0.4	> 0.4
$\eta(j_{f,1}) \cdot \eta(j_{f,2})$	< 0	< 0
$ \Delta\eta(j_{f,1}, j_{f,2}) $	> 4.2	> 4.2
$m_{jj_{ff}}$	> 750 GeV	> 750 GeV

ues. In addition to requiring at least four jets in the event topology, the VBF selection criteria requires two of those four jets have $p_T > 30$ GeV, $|\eta| < 5.0$, $|\Delta\eta_{jj_{ff}}| > 4.2$, $\eta_{j_{f,1}} \cdot \eta_{j_{f,2}} < 0$, and $m_{jj_{ff}} > 750$ GeV. Figure 4 shows the $|\Delta\eta_{jj_{ff}}|$ distribution in the $\tau_h\tau_h jjjj_{ff}$ channel, after requiring the central selections described above. Only the dijet pair with the largest $m_{jj_{ff}}$ is chosen to populate the distributions in Figure 4. Figure 5 shows the invariant dijet mass distribution, with the same criteria as in Figure 4. The VBF selection criteria is a powerful tool to reduce the contribution from $t\bar{t}$ (rejection power of 10^2) and Z/W +jets (rejection factors of 10^3 - 10^4). It is further noted that the QCD multijet background is not shown in those figures because it is found to be negligible with only the central selections (i.e. negligible yield after requiring six objects: two isolated leptons and four jets). However, VBF is also important to ensure the suppression of the QCD multijet background (10^4 suppression factor), which are typically relevant in final states with τ_h candidates due to the high jet- τ_h misidentification rate [24, 25]. Table I summaries the selections used in the $\mu\mu jjjj_{ff}$ and $\tau_h\tau_h jjjj_{ff}$ final states.

IV. RESULTS

The expected experimental sensitivity of each final state is determined using a binned-likelihood approach (i.e. a shape based analysis instead of a cut and count approach) following the test statistic based on the profile likelihood ratio, using the ROOTFit [34] toolkit. The

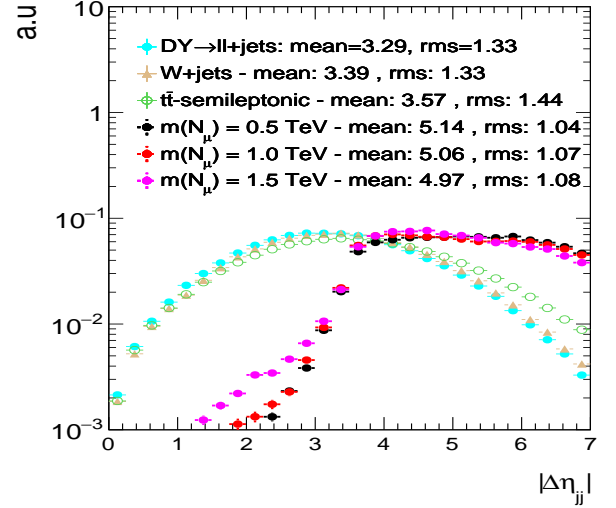


FIG. 4. Dijet $|\Delta\eta|$ distributions, normalized to unity, for the $\tau_h\tau_h jjjj_{ff}$ final state. The distributions are obtained after requiring at least two τ_h candidates with $p_T > 20$ GeV and $|\eta| < 2.1$.

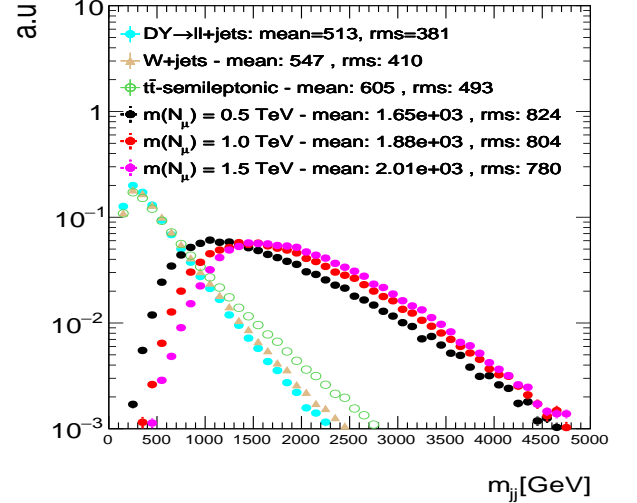


FIG. 5. Dijet mass distributions, normalized to unity, for the $\tau_h\tau_h jjjj_{ff}$ final state. The distributions are obtained after requiring at least two τ_h candidates with $p_T > 20$ GeV and $|\eta| < 2.1$, and two jets with $p_T > 30$ GeV, $|\eta| < 5.0$, $|\Delta\eta_{jj}| > 4.2$ and $m_{jj} > 500$ GeV.

sensitivity is determined using the “fit variable” that gives the best signal significance z . The signal significance is determined by first calculating a local p-value, defined as the the probability under a background only hypothesis to obtain a value of the test statistic as large as that obtained with a signal plus background hypothesis, and then extracting the value at which the integral of a Gaussian between z and ∞ results in a value equal to

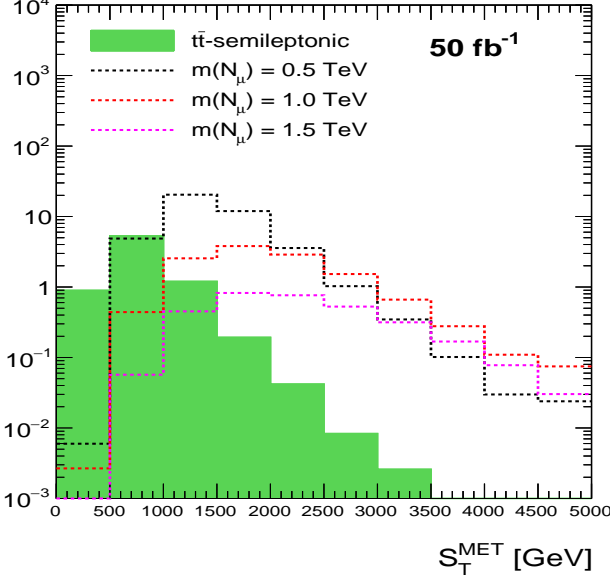


FIG. 6. S_T^{MET} distribution in the $\mu\mu jj jj jj_f$ final state, for the main backgrounds and two chosen signal benchmark points, after applying the final event selection criteria. The distributions are normalized to an integrated luminosity of 50 fb^{-1} .

the local p-value. Systematic uncertainties are incorporated via nuisance parameters following the frequentist approach. The dominant systematic uncertainties considered - τ_h identification (6%), VBF selection efficiency (20%), and the uncertainty due to the variations in the yields and shapes arising from the choice of parton distribution function (15%) - are based on available ATLAS and CMS results using τ_h candidates, muons, and/or the VBF topology [24, 25, 28–31, 35]. Based on these considerations, a total systematic uncertainty of 25% is applied on the signal and background yields. Several kinematic and topological variables, such as the missing transverse momentum p_T^{miss} , $m_{jj jj}$, H_T , S_T and S_T^{MET} , were considered as possible fit variables. The H_T variable is defined as the scalar sum of the p_T of all the jets in the event. The S_T variable is defined as the scalar sum of the H_T and the p_T of the two selected lepton candidates ($\tau_h\tau_h$ or $\mu\mu$ depending on the channel under consideration). The S_T^{MET} variable represents the scalar sum of the S_T and the p_T^{miss} variables. Using z as the figure of merit, the S_T^{MET} distribution provides the best expected sensitivity in both final states. Figures 6 and 7 show the S_T^{MET} distributions, after all of the event selection criteria outlined in Table I and normalized to an integrated luminosity of 50 fb^{-1} , for the $\mu\mu jj jj jj_f$ and the $\tau_h\tau_h jj jj jj_f$ search channels, respectively.

Figures 8 and 9 show the expected signal significance in the $\mu\mu jj jj jj_f$ and $\tau_h\tau_h jj jj jj_f$ channels, respectively, for integrated luminosities $L_{int} = 50\text{--}1000 \text{ fb}^{-1}$ and mixing $|V_{\ell N_\ell}|^2 = 1$. For $L_{int} = 100 \text{ fb}^{-1}$, the expected

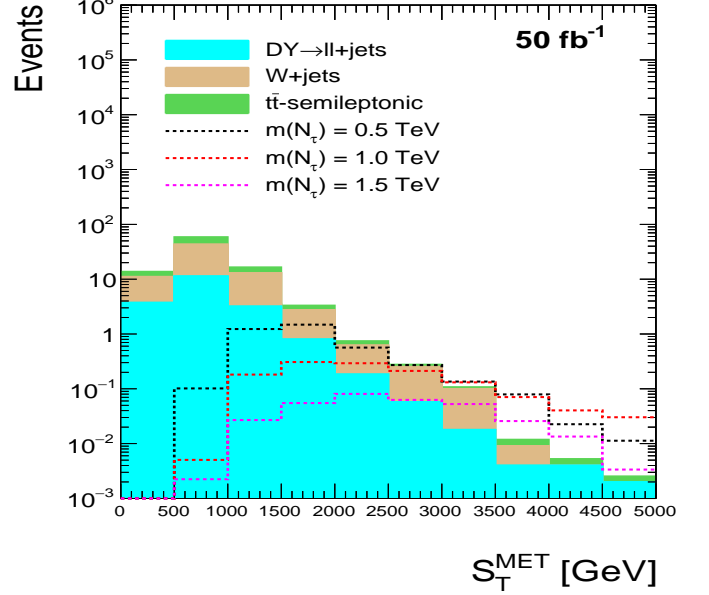


FIG. 7. S_T^{MET} distribution in the $\tau_h\tau_h jj jj jj_f$ final state, for the main backgrounds and two chosen signal benchmark points, after applying the final event selection criteria. The distributions normalized to an integrated luminosity of 50 fb^{-1} .

95% exclusion on m_{N_μ} using the $\mu\mu jj jj jj_f$ search channel is $\sim 1.7 \text{ TeV}$, while the 3σ (5σ) reach is ~ 1.3 (1.0) TeV. Similarly, the expected 95% exclusion on m_{N_τ} using the $\tau_h\tau_h jj jj jj_f$ search channel is $\sim 0.8 \text{ TeV}$ at $L_{int} = 100 \text{ fb}^{-1}$. For the longer-term projections of the high-luminosity LHC using $L_{int} = 1000 \text{ fb}^{-1}$, the expected 95% exclusion on m_{N_μ} (m_{N_τ}) using the $\mu\mu jj jj jj_f$ ($\tau_h\tau_h jj jj jj_f$) search channel is 2.4 (1.45) TeV, while the 3σ reach is ~ 2.05 (1.15) TeV. To highlight the importance of a N_ℓ search using the VBF topology, it is noted that the most recent search for N_τ [13] places no bound on m_{N_ℓ} beyond the LEP limit ($m_{N_\ell} < 0.1 \text{ TeV}$). As noted previously, this is because the current searches (non-VBF) for N_ℓ at ATLAS and CMS are optimized for resonant W_R^\pm production from DY processes ($pp \rightarrow W_R^\pm \rightarrow \ell N_\ell$) and assumes the mass is accessible at the LHC (i.e. the W_R mass is not too heavy). Existing results of the mTISM searches [11, 12], which are only performed in the electron and muon channels, exclude $m_{N_\ell} < 500 \text{ GeV}$ for $|V_{\ell N_\ell}|^2 = 1$. Therefore, a search for N_ℓ using VBF could be a complementary piece to the current N_ℓ search program at ATLAS and CMS, presenting a possible and important avenue for discovery.

We have optimized the selections/strategy outlined in this paper assuming the mixing between N_ℓ and ν_ℓ is unity ($|V_{\ell N_\ell}|^2 = 1$). However, our calculations can be generalized to scenarios with different mixing by appropriately scaling the expected signal yields. The event rate for N_ℓ detection at the LHC scales as $|V_{\ell N_\ell}|^2$, and

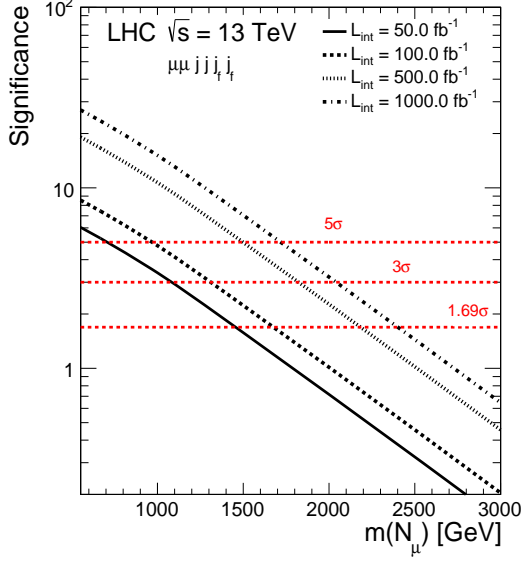


FIG. 8. Signal significance as a function of m_{N_μ} and L_{int} for the $\mu\mu jjjj$ search channel.

so smaller mixing leads to less sensitivity. Figure 10 shows the expected signal significance in the $\mu\mu jjjj$ and $\tau_h \tau_h jjjj$ channels, assuming an integrated luminosity of $L_{int} = 1000 \text{ fb}^{-1}$, considering different mixing scenarios. For $L_{int} = 1000 \text{ fb}^{-1}$ and $|V_{\ell N_\ell}|^2 = 10^{-1}$ ($|V_{\ell N_\ell}|^2 = 10^{-2}$), the expected 95% exclusion on m_{N_ℓ} is about 1.85 (1.0) TeV.

From Figures 6 and 7, it is clear that varying the rate and the shape of the S_T^{MET} distribution can be used to solve for the mass of N_ℓ as well as the mixing $|V_{\ell N_\ell}|^2$. The VBF N_ℓ study described in this paper was performed over a grid of input points in the m_{N_ℓ} - $|V_{\ell N_\ell}|^2$ plane, and the S_T^{MET} shape and expected rate in the search region were used to extract the measured m_{N_ℓ} and $|V_{\ell N_\ell}|^2$ values, including the expected uncertainties on those measurements. Figures 11 and 12 show how well m_{N_ℓ} and $|V_{\ell N_\ell}|^2$ can be measured as a function of integrated luminosity. For the signal benchmark scenario with $m_{N_\mu} = 500 \text{ GeV}$ and $|V_{\mu N_\mu}|^2 = 1$, Figure 11 shows that the heavy neutrino mass can be determined to within 30% (7%) accuracy, assuming $L_{int} = 50$ (1000) fb^{-1} . Similarly, the mixing can be determined to within 18% (4%) accuracy for an integrated luminosity of $L_{int} = 50$ (1000) fb^{-1} . In Figure 12 a benchmark signal sample with a lower mixing value of $|V_{\mu N_\mu}|^2 = 10^{-1}$ is considered. In Figure 13, the benchmark cases of $|V_{\mu N_\mu}|^2 = 1$ and $|V_{\mu N_\mu}|^2 = 10^{-1}$ were used to plot 1σ contours in the m_{N_μ} - $|V_{\mu N_\mu}|^2$ plane for an integrated luminosity of 1000 fb^{-1} at the 13 TeV LHC.

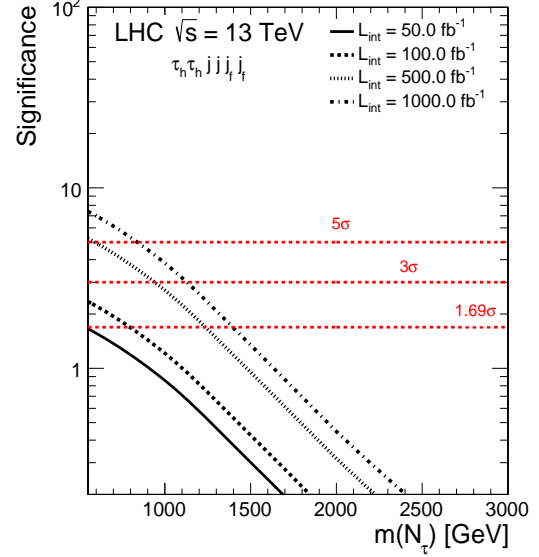


FIG. 9. Signal significance as a function of m_{N_τ} and L_{int} for the $\tau_h \tau_h jjjj$ search channel.

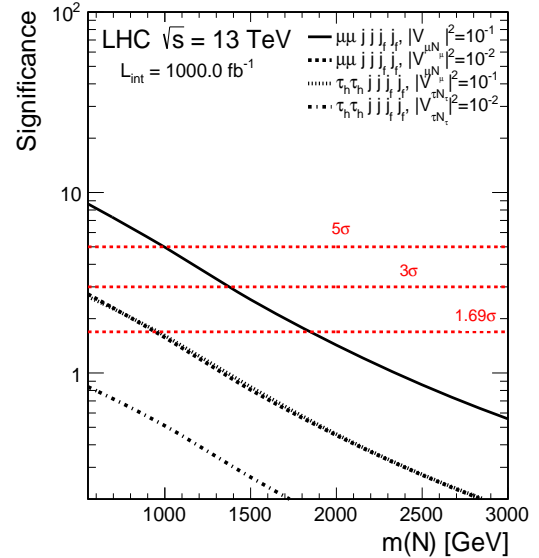


FIG. 10. Signal significance as a function of m_{N_ℓ} and mixing $|V_{\ell N_\ell}|^2$, assuming $L_{int} = 1000 \text{ fb}^{-1}$.

V. DISCUSSION

The main result of this paper is that searching for heavier neutrino states N_ℓ (predicted by extensions of the SM and inferred by the observation of neutrino oscillations) produced through VBF processes, can be a key method-

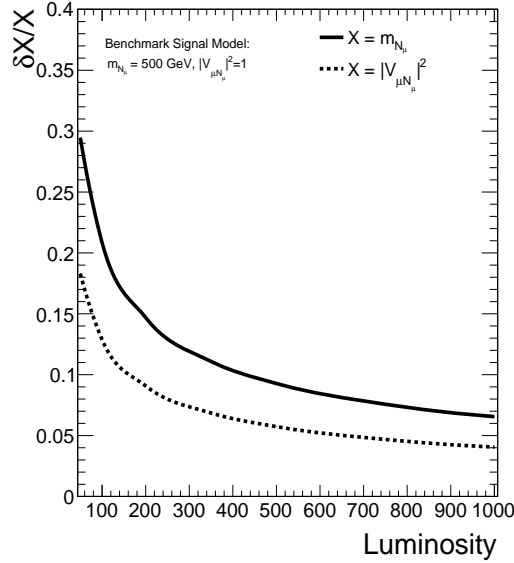


FIG. 11. Uncertainty on the measured heavy neutrino mass and mixing, as a function of integrated luminosity. The signal sample with $m_{N_\mu} = 500$ GeV and $|V_{\ell N_\mu}|^2 = 1$ is used as a benchmark.

ology to discover N_ℓ particles at the LHC. To highlight the expanded discovery reach, we consider N_ℓ production via VBF in the context of the mTISM and focus on the $\mu\mu jjjjjj$ and $\tau_h\tau_h jjjjjj$ channels to show that the requirement of a same-sign dilepton pair combined with two central jets and two additional high p_T forward jets with large separation in pseudorapidity and with large dijet mass is effective in reducing SM backgrounds. Assuming 100 fb^{-1} of 13 TeV proton-proton data from the LHC and mixing $|V_{\ell N_\ell}|^2 = 1$, the expected exclusion bounds (at 95% confidence level) are $m_{N_\mu} < 1.7$ TeV and $m_{N_\tau} < 0.8$ TeV in the $\mu\mu jjjjjj$ and $\tau_h\tau_h jjjjjj$ channels, respectively. These expected exclusion bounds with the VBF topology are to be compared to the current bounds of $m_{N_\mu} < 0.5$ TeV and $m_{N_\tau} < 0.1$ TeV. The use of the VBF topology to search for N_ℓ particles with TeV scale masses increases the discovery reach at the high-luminosity LHC, with signal significances greater than 5σ (3σ) for N_ℓ masses up to 1.7 (2.05) TeV and

0.9 (1.15) TeV in the $\mu\mu_h jjjjjj$ and $\tau_h\tau_h jjjjjj$ channels, assuming $L_{int} = 1000 \text{ fb}^{-1}$. It has been shown that broad enhancements in the S_T^{MET} distributions after VBF selections provide a smoking gun signature for VBF production of N_ℓ . By simultaneously fitting the S_T^{MET} shape and observed rate in data, the mass and mixing can be measured to within 7% and 4% accuracy for an integrated luminosity of 1000 fb^{-1} at the 13 TeV LHC.

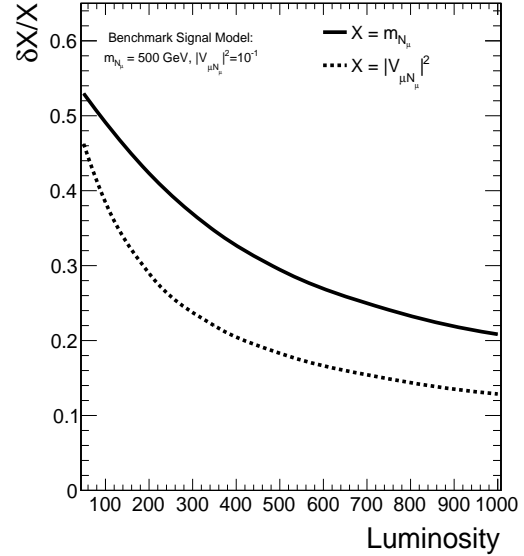


FIG. 12. Uncertainty on the measured heavy neutrino mass and mixing, as a function of integrated luminosity. The signal sample with $m_{N_\mu} = 500$ GeV and $|V_{\ell N_\ell}|^2 = 10^{-1}$ is used as a benchmark.

VI. ACKNOWLEDGEMENTS

We thank the constant and enduring financial support received for this project from the faculty of science at Universidad de los Andes (Bogotá, Colombia), the faculty of science at Universidad de Antioquia, the administrative department of science, technology and innovation of Colombia (COLCIENCIAS), the Physics & Astronomy department at Vanderbilt University and the US National Science Foundation. This work is supported in part by NSF Award PHY-1506406.

-
- [1] G. Aad *et al.* [ATLAS Collaboration], “Observation of a new particle in the search for the Standard Model Higgs boson with the ATLAS detector at the LHC,” *Phys. Lett. B* **716**, 1, 1-29 (2012) 10.1016/j.physletb.2012.08.020 [arXiv:1207.7214 [hep-ex]].
- [2] V. Khachatryan *et al.* [CMS Collaboration], “Observation of a new boson at a mass of 125 GeV with the CMS

experiment at the LHC,” *Phys. Lett. B* **716**, 1, 30-61 (2012) 10.1016/j.physletb.2012.08.021 [arXiv:1207.7235 [hep-ex]].

- [3] Y. Fukuda *et al.* [Super-Kamiokande Collaboration], “Evidence for oscillation of atmospheric neutrinos,” *Phys. Rev. Lett.* **81**, 1562 (1998) doi:10.1103/PhysRevLett.81.1562 [hep-ex/9807003].

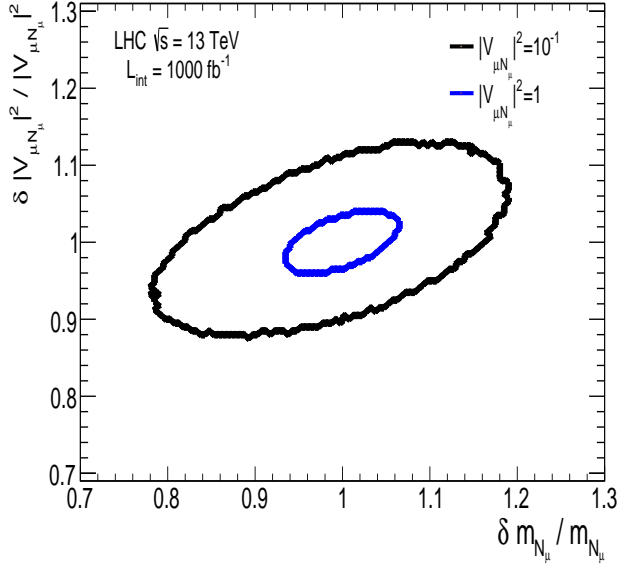


FIG. 13. 1σ contour lines in the m_{N_μ} - $|V_{\mu N_\mu}|^2$ plane for the signal benchmark scenario with $m_{N_\mu} = 500$ GeV and $L_{int} = 1000 \text{ fb}^{-1}$.

- [4] Q. R. Ahmad *et al.* [SNO Collaboration], “Measurement of the rate of $\nu_e + d \rightarrow p + p + e^-$ interactions produced by ^8B solar neutrinos at the Sudbury Neutrino Observatory,” *Phys. Rev. Lett.* **87**, 071301 (2001) doi:10.1103/PhysRevLett.87.071301 [nucl-ex/0106015].
- [5] Q. R. Ahmad *et al.* [SNO Collaboration], “Direct evidence for neutrino flavor transformation from neutral current interactions in the Sudbury Neutrino Observatory,” *Phys. Rev. Lett.* **89**, 011301 (2002) doi:10.1103/PhysRevLett.89.011301 [nucl-ex/0204008].
- [6] M. Lindner, T. Ohlsson and G. Seidl, “Seesaw mechanisms for Dirac and Majorana neutrino masses,” *Phys. Rev. D* **65**, 053014 (2002) doi:10.1103/PhysRevD.65.053014 [hep-ph/0109264].
- [7] P. Minkowski, “ $\mu \rightarrow e\gamma$ at a Rate of One Out of 10^9 Muon Decays?,” *Phys. Lett.* **67B**, 421 (1977). doi:10.1016/0370-2693(77)90435-X
- [8] R. N. Mohapatra and G. Senjanovic, “Neutrino Mass and Spontaneous Parity Violation,” *Phys. Rev. Lett.* **44**, 912 (1980). doi:10.1103/PhysRevLett.44.912
- [9] S. Chatrchyan *et al.* [CMS Collaboration], “The CMS experiment at the CERN LHC,” *JINST* **3**, S08004 (2008). doi:10.1088/1748-0221/3/08/S08004
- [10] G. Aad *et al.* [ATLAS Collaboration], “The ATLAS Experiment at the CERN Large Hadron Collider,” *JINST* **3**, S08003 (2008). doi:10.1088/1748-0221/3/08/S08003
- [11] G. Aad *et al.* [ATLAS Collaboration], “Search for heavy neutrinos and right-handed W bosons in events with two leptons and jets in pp collisions at $\sqrt{s} = 7$ TeV with the ATLAS detector,” *Eur. Phys. J. C* **72**, 2056 (2012) doi:10.1140/epjc/s10052-012-2056-4 [arXiv:1203.5420 [hep-ex]].
- [12] V. Khachatryan *et al.* [CMS Collaboration], “Search for heavy neutrinos and W bosons with right-handed couplings in proton-proton collisions at $\sqrt{s} = 8$ TeV,” *Eur. Phys. J. C* **74**, no. 11, 3149 (2014) doi:10.1140/epjc/s10052-014-3149-z [arXiv:1407.3683 [hep-ex]].
- [13] V. Khachatryan *et al.* [CMS Collaboration], “Search for heavy neutrinos or third-generation leptoquarks in final states with two hadronically decaying τ leptons and two jets in proton-proton collisions at $\sqrt{s} = 13$ TeV,” *JHEP* **1703**, 077 (2017) doi:10.1007/JHEP03(2017)077 [arXiv:1612.01190 [hep-ex]].
- [14] B. Dutta, A. Gurrola, W. Johns, T. Kamon, P. Sheldon and K. Sinha, “Vector Boson Fusion Processes as a Probe of Supersymmetric Electroweak Sectors at the LHC,” *Phys. Rev. D* **87**, no. 3, 035029 (2013) doi:10.1103/PhysRevD.87.035029 [arXiv:1210.0964 [hep-ph]].
- [15] A. Delannoy *et al.*, “Probing Dark Matter at the LHC using Vector Boson Fusion Processes,” *Phys. Rev. Lett.* **111**, 061801 (2013) doi:10.1103/PhysRevLett.111.061801 [arXiv:1304.7779 [hep-ph]].
- [16] B. Dutta, T. Ghosh, A. Gurrola, W. Johns, T. Kamon, P. Sheldon, K. Sinha and S. Wu, “Probing Compressed Sleptons at the LHC using Vector Boson Fusion Processes,” *Phys. Rev. D* **91**, 055025 (2015) 10.1103/PhysRevD.91.055025 [arXiv:1411.6043 [hep-ph]].
- [17] B. Dutta, W. Flanagan, A. Gurrola, W. Johns, T. Kamon, P. Sheldon, K. Sinha, K. Wang and S. Wu, “Probing Compressed Top Squarks at the LHC at 14 TeV,” *Phys. Rev. D* **90**, 095022 (2014) 10.1103/PhysRevD.90.095022 [arXiv:1312.1348 [hep-ph]].
- [18] B. Dutta *et al.*, “Probing Compressed Bottom Squarks with Boosted Jets and Shape Analysis,” *Phys. Rev. D* **92**, 095009 (2015) 10.1103/PhysRevD.92.095009 [arXiv:1507.01001 [hep-ph]].
- [19] A. Flrez, A. Gurrola, W. Johns, Y. D. Oh, P. Sheldon, D. Teague and T. Weiler, “Searching for New Heavy Neutral Gauge Bosons using Vector Boson Fusion Processes at the LHC,” *Phys. Lett. B* **767**, 126 (2017) doi:10.1016/j.physletb.2017.01.062 [arXiv:1609.09765 [hep-ph]].
- [20] J. Alwall *et al.*, “The automated computation of tree-level and next-to-leading order differential cross sections, and their matching to parton shower simulations,” *JHEP* **1407**, 079 (2014) doi:10.1007/JHEP07(2014)079 [arXiv:1405.0301 [hep-ph]].
- [21] T. Sjostrand, S. Mrenna and P. Z. Skands, *J. High Energy Phys.* **0605**, 026 (2006) [hep-ph/0603175].
- [22] J. de Favereau *et al.* [DELPHES 3 Collaboration], “DELPHES 3, A modular framework for fast simulation of a generic collider experiment,” *JHEP* **1402**, 057 (2014) doi:10.1007/JHEP02(2014)057
- [23] J. Alwall *et al.*, “Comparative study of various algorithms for the merging of parton showers and matrix elements in hadronic collisions,” *Eur. Phys. J. C* **53**, 473 (2008) doi:10.1140/epjc/s10052-007-0490-5, arXiv:0706.2569.
- [24] V. Khachatryan *et al.* [CMS Collaboration], “Search for supersymmetry in the vector-boson fusion topology in proton-proton collisions at $\sqrt{s} = 8$ TeV,” *JHEP* **1511**, 189 (2015) doi:10.1007/JHEP11(2015)189 [arXiv:1508.07628 [hep-ex]].
- [25] V. Khachatryan *et al.* [CMS Collaboration], “Search for dark matter and supersymmetry with a compressed mass spectrum in the vector boson fusion topology in proton-proton collisions at $\sqrt{s} = 8$ TeV,” *Phys. Rev. Lett.* **118**,

- 021802 (2017). doi:10.1103/PhysRevLett.118.021802
- [26] L. Randall and R. Sundrum, Phys. Rev. Lett. **83**, 3370 (1999) doi:10.1103/PhysRevLett.83.3370 [hep-ph/9905221].
- [27] M. Cvetič, and S. Godfrey, “Discovery and Identification of Extra Gauge Bosons,” OCIP/C-95-2, UPR-648-T [arXiv:hep-ph/9504216].
- [28] G. Aad *et al.* [ATLAS Collaboration], “A search for high-mass resonances decaying to $\tau^+\tau^-$ in pp collisions at $\sqrt{s} = 8$ TeV with the ATLAS detector,” JHEP **07**, 157 (2015). 10.1007/JHEP07(2015)157 [arXiv:1502.07177 [hep-ex]].
- [29] V. Khachatryan *et al.* [CMS Collaboration], “Search for new physics with high-mass tau lepton pairs in pp collisions at $\sqrt{s} = 13$ TeV with the CMS detector,” JHEP **02**, 048 (2017) doi:10.1007/JHEP02(2017)048 [arXiv:1611.06594 [hep-ex]].
- [30] G. Aad *et al.* [ATLAS Collaboration], “Search for new high-mass resonances in the dilepton final state using proton-proton collisions at $\sqrt{s} = 13$ TeV with the ATLAS detector,” ATLAS-CONF-2016-045.
- [31] V. Khachatryan *et al.* [CMS Collaboration], “Search for a high-mass resonance decaying into a dilepton final state in 13 fb $^{-1}$ of pp collisions at $\sqrt{s} = 13$ TeV,” CMS-PAS-EXO-16-031.
- [32] V. Khachatryan *et al.* [CMS Collaboration], “Search for high-mass diphoton resonances in proton-proton collisions at 13 TeV and combination with 8 TeV search,” Phys. Lett. B **767**, 147 (2017) doi:10.1016/j.physletb.2017.01.027 [arXiv:1609.02507 [hep-ex]].
- [33] M. Aaboud *et al.* [ATLAS Collaboration], “Search for resonances in diphoton events at $\sqrt{s}=13$ TeV with the ATLAS detector,” JHEP **1609**, 001 (2016) doi:10.1007/JHEP09(2016)001 [arXiv:1606.03833 [hep-ex]].
- [34] L. Moneta, K. Belasco, K. S. Cranmer, S. Kreiss, A. Lazzaro, et. al., The RooStats Project, PoS ACAT2010 (2010) 057, [1009.1003]
- [35] V. Khachatryan *et al.* [CMS Collaboration], “Performance of τ -lepton reconstruction and identification in CMS,” J. Instrum. **07**, P01001 (2012) doi:10.1088/1748-0221/7/01/P01001 [arXiv:109.6034 [hep-ex]].
- [36] C. Hill, “Topcolor Assisted Technicolor,” Phys. Lett. B **345**, 483-489 (1995). doi:10.1016/0370-2693(94)01660-5